ELSEVIER

Thermochimica Acta 388 (2002) 389–400

thermochimica acta

www.elsevier.com/locate/tca

Kinetic evaluation of DSC curves for reacting systems with variable stoichiometric compositions

Hans-Jürgen Flammersheim[a,*], Johannes R. Opfermann[b]

[a]*Institut für Physikalische Chemie, Friedrich-Schiller-Universität Jena, Lessingstraße 10, D-07743 Jena, Germany*
[b]*NETZSCH-Gerätebau GmbH, Wittelsbacherstraße 42, D-95100 Selb, Germany*

Received 25 May 2001; received in revised form 15 August 2001; accepted 19 August 2001

Abstract

At present, the most popular programs for kinetic evaluation of reaction curves obtained by thermal analysis methods do not allow simultaneous analysis of systems with different stoichiometry. Consequently, valid predictions of the reaction behavior are limited to fixed compositions that have been investigated. Further, mechanistic conclusions should be taken with greatest caution if at all. The main aim of the new program is to determine the kinetic parameters for all (important) steps of an assumed and most probable reaction mechanism on the basis of differential scanning calorimetry (DSC) measurements and, of course, using these results to predict the reaction behavior for any complex temperature-time profile. Even if the reaction mechanism is not too complex, this can be done only if the experimental information is adequate. Therefore, besides having a sufficient reaction window (isothermal reaction temperatures and/or heating rates) the initial composition of the reaction mixture should also be varied as widely as possible. It is then possible to check the compatibility of the assumed reaction mechanism with the measured DSC curves. The new program was not developed to replace formal-kinetic evaluations but it is a valuable supplementary tool for kinetic evaluations. As a rule, results from other analytical methods must be considered in defining an adequate kinetic model, even if only the relevant elementary steps of the assumed mechanism are considered. The structure of the new evaluation program "Component kinetics" and a number of typical applications are discussed.

Keywords: DSC; Kinetics; Reaction mechanism; Evaluation program; Non-linear regression

1. Introduction

At present, kinetic evaluation methods can be differentiated in the following three large groups:

1. Traditional methods try to describe the results of kinetic experiments by systematically testing the known rate laws for reactions in homogeneous or hetero-geneous phases. This is frequently carried out by restricting the range of conversion degree.

Another possibility is the use of so-called overall rate laws, which are derived from a probable but often strongly simplified mechanism. A typical example is the Sourour–Kamal Eq. (1), which was originally derived by Smith [2] for epoxide-amine polyaddition reactions in dilute solutions.

$$\frac{d\alpha}{dt} = (k_1 + k_2\alpha^m)(1-\alpha)^n \quad (1)$$

where α is the extent of reaction, k_1 and k_2 the rate constants for the catalysed and autocatalysed reactions, n and m the partial reaction orders, t the time.

* Corresponding author. Fax: +49-3641-948302.
E-mail address: c7flha@uni-jena.de (H.-J. Flammersheim).

0040-6031/02/$ – see front matter
PII: S0040-6031(02)00042-4

As a rule, solvent-free reactions can be described only for low conversion ranges when $n = 2$ and $m = 1$. The use of n and m as freely optimized and temperature-dependent parameters [3–5] increases the range of validity, but now completely loses connection with the chemistry of the process.

In the past isothermal measurements were the rule, resulting from the limited performance of differential scanning calorimetry (DSC) devices, computerisation and evaluation programs. Due to the small temperature range which was accessible, the obtained kinetic parameters were uncertain, especially for more complex reactions.

2. Modern, highly sensitive DSC devices, powerful computerisation and sophisticated evaluation methods, both allow and favor the combined realisation and evaluation of isothermal and non-isothermal experiments.

   Model-free methods allow evaluation of the Arrhenius parameters without choosing the reaction model. The best known approaches, if several measurements with different heating-rates and/or with different temperatures have been made, are the differential isoconversional method according to Friedman [6] and the integral isoconversional method according to Ozawa [7] and Flynn and Wall [8]. Assuming the simple additive superposition of the individual reactions for a possible multi-step mechanism, the expansion of the integral isoconversional technique according to Vyazovkin [9] also permits predictions of the reaction behavior for isothermal conditions.

   However, the greatest caution should be taken when coming to mechanistic conclusions as a result of possibly detected dependence $E_A = f(\alpha)$, where E_A is the Arrhenius activation energy.

3. Another possibility is the description of the reaction behavior by a formal-kinetic model [10–12]. This is probably, at present, the most flexible, simple and fastest solution concerning the fitting of reaction curves. Using the vocabulary and basic ideas of usual reaction kinetics, the overall reaction is described by the combination of formal reaction steps (independent, parallel, competitive or consecutive) with constant activation parameters. As a rule, these steps may not be interpreted as existing chemical reactions. A high value of the fitting quality for the best model does not mean that the kinetic description [13] is correct in the physicochemical meaning! But the industrial practitioner is usually more interested in predictions of the reaction behavior for arbitrary temperature-time profiles, than knowing or understanding the real mechanism. As with the model-free analysis, the knowledge of the composition of the reacting system is not necessary.

The most common disadvantages of all these techniques result from the fact that the obtained process parameters and the derived conclusions are valid only for the tested composition of the reaction mixture. To be more exact, we have two disadvantages: technically important reaction mixtures could have different amounts of catalysts, non-reactive fillers or solvents; and, in addition, if the stoichiometric composition of the reaction mixture cannot be varied, then important additional information concerning the verification, acceptance or rejection of an assumed reaction mechanism is not available. This is true for such cases, in which one or several elementary steps of the mechanism are influenced only by a specific reactant. Our aim was the development of a program which is easy to operate and which has the following attributes:

- Unrestricted combination of elementary steps (consecutive, parallel, equilibrium).
- Simultaneous evaluation of both isothermal and non-isothermal measurements.
- Simultaneous evaluation of curves for mixtures with variable compositions and differing amounts of reactive (catalysts) and non-reactive (fillers, solvents) substances.
- Consideration of changes in volume during the reaction.
- Test of significance regarding the fitting quality of different models and regarding an assumed number of reaction steps.
- Predictions for signal, fractional reaction and reactants for any temperature-time-program.

2. Description of the software package

The necessary input data are the DSC curves, the initial concentrations of all constituents of the reaction mixture and the assumed reaction steps together with

their initial values for Arrhenius parameters and reaction heats. The most important steps and actions are described now in detail and in the same order, that is necessary to treat a kinetic problem:

1. The number of curves to be evaluated simultaneously in the planned project must be defined. The maximum number is 16, which should be sufficient for scanning an adequate range within the global reaction field [14]. Single heating-rate curves are useless for a kinetic analysis [14,15]. The heating-rates to be used should vary at least by one-order of magnitude; the temperature range of isothermal measurements and the variation of the initial composition should be as large as possible.
2. After loading the DSC curves, the measurements are desmeared and smoothed if required. The system function for the deconvolution of the original curves is obtained from the tail of a melting peak, using a pure sample with comparable heat conductivity and heat capacity. This also corrects any sample self-heating during the exothermic reaction.
3. There are several possibilities (linear, sigmoidal, left-starting, right-starting) of constructing the baseline between the chosen limits of peak integration. A 'zero'-baseline is, without doubt, the best alternative if the DSC scan has already been corrected with an independently measured base line, such as the ''reversing'' signal from a temperature modulated DSC.
4. Next, the supposed reaction mechanism as a sequence of all elementary steps is formulated. Reversible reactions with very high rate constants for both forward and backward reactions can be formulated as equilibrium reactions. This reduces the number of parameters to be determined and avoids the necessity of solving stiff differential equation systems. Of course, using only the overall DSC curves, it is rarely possible to determine significant model parameters of more than three or four reactions. This is even true if 16 curves with extensively varied compositions and measuring conditions (resulting in a large range of the global reaction field) are evaluated simultaneously. However, sometimes additional information is available from other analytical techniques, for example, the equilibrium constants of some steps and, with this additional information, it is then possible to define a more complex model. Therefore, this program allows a maximum of 12 elementary steps. Using symbolic letters or short names for the reactants, the reaction mechanism can be formulated as usual in chemistry. The same input window can also be used to enter the molar masses and the specific densities of all reactants, including those of a possible solvent.
5. Molar masses and densities are valid for all curves of the chosen model, while the stoichiometric composition of the reaction mixture can be different for each curve. The molar masses are needed in order to calculate the start concentrations. Normally, the initial weights of all components of the respective scan are entered. Alternatively, the start concentrations can be inputted. The program checks the mass balance.
6. In the next step, usable initial values are needed for all variables of the kinetic scheme, for elementary reactions $\log A$, E_A and Q_r, for equilibrium reactions $\Delta_r H$ and $\Delta_r S$ (A is the Arrhenius pre-exponential factor, Q_r the reaction heat, $\Delta_r H$ and $\Delta_r S$ the reaction enthalpy and entropy). The consistency of the reaction heats is checked according to Hess' law. If no further information is available, a clue to such values may sometimes be obtained from the model-free evaluation. This is shown in Fig. 1 with the example of two independent parallel reactions (case 3b in Table 1) on the basis of 12 scans. The used isoconversional method according to Ozawa–Flynn–Wall is available as subroutine in the ''NETZSCH Thermokinetics'' program [14]. This program uses the words ''partial area'' instead of ''extent of reaction'' as the label on the x-axis. Because only the partial area value, calculated from DSC measurements for single step reactions, and the chemically defined extent of reaction are necessarily identical. Quite obviously, the function $E_A = f(\alpha)$ or more correctly $E_A = f(\text{partial area})$ also depends on the initial stoichiometry of the reaction mixture. The results presented in Fig. 1 underline again that a mechanistic interpretation of such results is ambiguous or impossible. Despite this, the model-free analysis clearly shows that at least two elemental steps must be

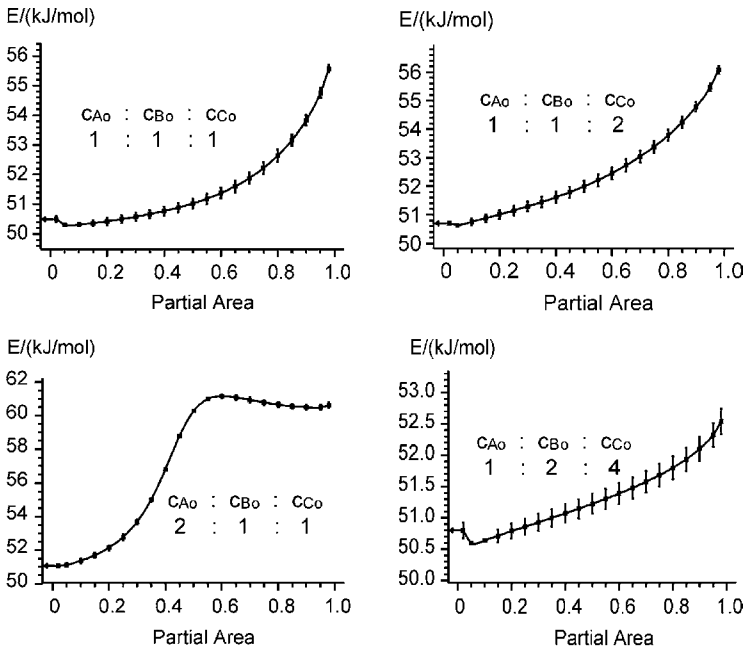

Fig. 1. Estimation of starting values for the non-linear regression using the model-free isoconversional method according to Ozawa–Flynn–Wall. Example, different initial stoichiometries for the mechanism with two independent parallel reactions.

Table 1
List of the most important, tested projects using faultless simulated DSC curves. In each project heating-rates, isothermal temperatures and stoichiometric compositions were varied

Case type	$n = 2$, $\log A(s^{-1}\,l\,mol^{-1})$ $n = 1$, $\log A/(s^{-1})$	E_A(kJ mol^{-1})	Q_r(kJ mol^{-1})	$\Delta_r S^{\neq}$(J K mol^{-1})	$\Delta_r H^{\neq}$(kJ mol^{-1})
1 Simple *n*th-order					
A + B→C	5.0	50.0	−37.0		
2 Autocatalytical					
A + B→ C + 2B	13.0	100.0	−10.0		
3 Parallel					
a) A→X	19.222	300.0	−100.0		
A→Y	4.222	100.0	−100.0		
b) A + B→X	5.0	50.0	−50.0		
A + C→Y	5.5	60.0	−100.0		
4 Subsequent					
a) A→X	19.222	300.0	−100.0		
X→Y	4.222	100.0	−100.0		
b) A + B→X	5.0	50.0	−50.0		
X + C→Y	5.5	60.0	−100.0		
5 Pre-equilibria					
a) A + K↔AK	–	–	–	−10.36	21.6
AK + B→C + 2 K	4.06	56.0	−5.0	–	–
b) E + OH↔EOH	–	–	–	−2.964	–
P + OH ↔ POH	–	–	–	−8.044	–
EOH + P→S + 2 OH	4.57	55.7	−108.0	–	–
EOH + POH→S + 3 OH	3.54	44.7	−108.0		–
E + 2 P →S + OH + P	3.87	70.0	−108.0		–

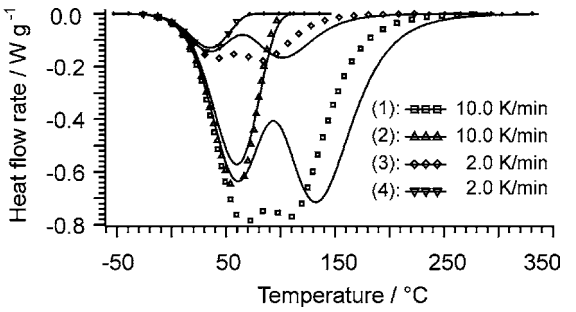

Fig. 2. Optical adjustment of the starting values ($E_{A1} = 50\,kJ\,mol^{-1}$, $E_{A1} = 60\,kJ\,mol^{-1}$) obtained according Fig. 1 and estimation of the pre-exponentials ($\log A_1 = \log A_2 = 5\,s^{-1}\,l\,mol^{-1}$) in the subroutine "visual optimisation". Curves (1) and (3), c_{A0}:c_{B0}:c_{C0} = 2:1:1; curves (2) and (4), c_{A0}:c_{B0}:c_{C0} = 1:2:4.

considered. If, by comparison with Fig. 1, the two activation energies are taken as being 50 and 60 kJ mol^{-1} (using the correct model), then the starting situation shown in Fig. 2 is achieved. The different symbols mark the "experimental" curves and the solid lines correspond to the calculated curves. For the sake of the clarity, only four of the 12 curves used have been shown. The quality of this fit can be adjusted and improved by trial and error, using the sub-routine "visual optimisation". The initial values for the pre-exponentials ($\log A_1 = \log A_2 = 5\,s^{-1}\,l\,mol^{-1}$) were obtained in this manner. It is extremely important to find meaningful initial values for the subsequent non-linear optimisation.

7. The differential equation solver used is a combination of embedded Prince–Dormand procedure of 4/5 degree with a Gear4 procedure [16]. In the Prince–Dormand procedure two checks regarding stiffness have been integrated. The calculation always starts with the Prince–Dormand procedure. If both checks regarding stiffness are positive, then the calculation continues using the Gear4 procedure. There are three criteria to terminate the iterations. The first criterion is an inherent part of the algorithm and causes the iterations to finish automatically, if the relative change of all parameter values is lower than a defined precision. User-defined criteria are the number of iterations or a maximum value of the correlation coefficient. It is well known that the speed of optimisation is reduced by the so-called thermal compensation effect. A special mathematical subroutine suggested by Benoit et al. [17] ensures that the iterations go straight to the optimum parameters of the tested mechanism. The correlation between $\log A$ and E_A is temporarily reduced by means of the following transformation:

$$\log A = \log A^* - \frac{E_A}{RT_{mean}}$$

where T_{mean} is the mean value of the inverse temperatures within the analysis range.

For instance, starting with the kinetic parameters used in Fig. 2, a perfect fit and the theoretical values are reached in only four iteration cycles. The results are the optimal parameters for all variables including their standard deviations and some specifications concerning the statistical analysis (sum of least squares, correlation coefficient, mean residues, Durbin–Watson value). A very useful tool is the *F*-test [14], which enables one to decide whether a tested model is significantly better suited for the characterisation of the measurements than another one. Finally, a step-significance *F*-test is similarly valuable. It answers the question of whether an additional step yields not only a better fit but also a statistically significant improvement of the model.

8. Predictions of the reaction behavior can be made for any complex temperature-time profile using the favored model and its parameters. These predictions concern the concentration behavior of all reactants and products, the DSC signal and the partial area "degree of conversion".

3. Results and discussion of some typical examples

3.1. Simulated, error-free data

The primary task was, of course, to prove that the program operates correctly for all possible combinations of elementary reactions in homogeneous kinetics. Therefore, we first calculated theoretical, error-free heat flow curves for the following reaction types:

1. A simple second-order reaction.
2. An autocatalytic second-order reaction.

3. Two first -or second-order parallel reactions.
4. Two consecutive reactions with first -or second-order.
5. Several types of pre-equilibria coupled with consecutive and parallel reactions. Both temperature dependent ($\Delta H^{\neq} \neq 0$) and independent ($\Delta H^{\neq} = 0$) equilibrium constants were assumed by us.

Table 1 summarises some selected cases. Each parameter set should, in principle, be suitable, in order to test the performance of the new program. The used values for $\log A$ and E_A are not unusual for chemical reactions. Similarly to the intention of the ''ICTAC Kinetics Project, 2000'' ([18], p. 157) regarding the simulated data, the Arrhenius parameters of the individual steps for the cases three and four were chosen to make the rates of the two steps comparable. The assumed temperature dependence of the pre-equilibrium for case 5a corresponds to the temperature dependence of the hydrogen iodide equilibrium between 300 and 700 K. For case 5b, we have used parameters which are frequently found for epoxide amine reactions. On the basis of each assumed reaction mechanism, we have calculated non-isothermal curves, using heating rates of 0.5, 2.0 and 10.0 K min^{-1}, and also a number of isothermal curves. The selection of appropriate temperatures is also governed by the same rule-of-thumb which is recommended for real experiments. They should cover the first half of the leading edge of the temperature programmed scan with low heating rates (0.5–2 K min^{-1}). The selection criterion for isothermal measurements is fully explained in the context of the Figs. 4 and 5. Further, the starting concentrations of the components, in comparison to the equimolar mixture, were always strongly varied up to a fourfold excess of one component. For example, for cases 3b and 4b in Table 1 that means c_A:c_B:c_C = 1:1:4, 1:4:1, 4:1:1, 1:4:4, 4:4:1 and 4:1:4. Of course, the complete combination of all concentration ratios with all scanning rates and isothermal temperatures is neither necessary nor useful (information content, capacity of the evaluation program, calculating time). Frequently, it was additionally simulated that the curves belong to mixtures with different amounts of solvent. Finally, we have calculated theoretical curves assuming different densities for reactants and products.

Without exception, the separate or simultaneous evaluation of isothermal and non-isothermal scans exactly reproduced all values of the pre-exponential factors, the activation energies, the equilibrium constants and the reaction heats used in calculating the theoretical curves. That means, the new program enables both the correct identification of the reaction mechanism and the determination of its parameters, at least in these relatively simple cases.

3.2. Consideration of typical sources of error using DSC measurements

Next, we have simulated two second-order consecutive reactions and added typical sources of error in real DSC measurements as well as noise and base-line shift. The results are summarised in Table 2. First, we have superimposed the error-free curves with a random noise of ±10 μW. This can be taken as the worst condition for non-isothermal measurements in modern DSC's. Table 2 shows that the calculated model parameters are not influenced. That means, the evaluation of real, noisy curves instead of perfectly smooth simulated data is irrelevant as source of error.

Table 2
Project: two second-order consecutive reactions. Influence of noise and base-line shifts superimposed onto faultless simulated DSC curves. The standard deviations for the kinetic parameters in the columns three and four are negligible

	Preset values	Faultless curves	Noisy curves	Noise plus shift weighting: 1	Noise plus shift weighting:1/[abs(Y_{max}) + abs(Y_{min})]
$\log A_1$ (s^{-1} l mol^{-1})	5	5	5.002	4.97 ± 0.02	4.97 ± 0.02
E_{A1} (kJ mol^{-1})	50	50	50.01	49.78 ± 0.10	49.81 ± 0.07
Q_{r1} (kJ mol^{-1})	−50	−50	−50	−50.78 ± 0.10	−50.65 ± 0.10
$\log A_2$ (s^{-1} l mol^{-1})	5.5	5.5	5.501	5.57 ± 0.02	5.55 ± 0.02
E_{A2} (kJ mol^{-1})	60	60	60.01	60.48 ± 0.08	60.29 ± 0.06
Q_{r2} (kJ mol^{-1})	−100	−100	−99.99	−99.13 ± 0.12	−99.27 ± 0.10

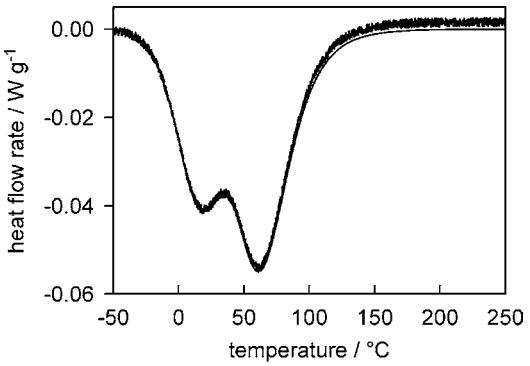

Fig. 3. Comparison of an error-free (smooth line) theoretical curve and of the same curve superimposed by an additional noise of 10 μW and a conversion–proportional shift of 0.2 mW (dashed line). Example, two consecutive second-order reactions, compare Table 1.

Secondly, we have also assumed undetected and therefore uncorrected base line shifts and/or curvatures due to either noticeable changes of the reaction heat capacity or to changes of heat transfer and thermal conductivities. For this, we have superimposed the noisy curves with a sigmoidal shift of 0.2 mW, proportional to the degree of conversion. This superposition is shown in Fig. 3 as an example of a non-isothermal run at 0.5 K min^{-1}, assuming model and model parameters for two subsequent second-order reactions (example 4a in Table 1). Even at this low heating rate, the differences between the undisturbed, noise-free curve (the smooth curve in Fig. 3) and the superpositioned curve are very small. Neglecting the modified shape, the baseline was then taken as linear connection between start and end point of the scan. Table 2 shows that the model parameters are still reproduced with sufficient accuracy but that systematic deviations from the true values and clearly larger standard deviations are already present. Uncertainties concerning the exact course of the base line are still an inherent weakness of DSC measurements. This simple example emphasises that kinetic evaluations are trustworthy only for high-quality measurements. The least that an experimenter should do, is to repeat measurements using the same conditions, if possible coupled with independent estimations of the heat capacities for reactants and products. If a temperature modulated DSC is available, one should use this technique to separate the overall signal in its ''kinetic'' and ''thermodynamic'' components [19].

Kinetic experiments can be made isothermally or non-isothermally. Both modes are possible in DSC and have both advantages and disadvantages. They complement each other and should not be regarded as alternatives [20]. The specific advantage of isothermal measurements is sometimes the simple and immediate qualitative interpretation of the measured curve due to the complete decoupling of the two variables, temperature and time. The main disadvantages are the uncertainties of the signal during the initial and the final phase. Contrary to this, a non-isothermal measurement can be started at a temperature well below that of the beginning of the reaction with a small reaction rate. Also, the reactions are completed within a finite time. In each case, the simultaneous kinetic evaluation of isothermal and non-isothermal scans is not only possible but is highly recommended to avoid misinterpretations. A necessary pre-condition is, however, that the reaction field covered by the experiments is sufficient. This requirement is easily fulfilled by carrying out non-isothermal measurements using a variation of heating rates by one-order of magnitude. The following examples show that the situation is much more difficult when using isothermal experiments.

We want to demonstrate the above with a first favorable example that an autocatalytic reaction takes place, as frequently found in epoxy curing reactions [1,2,21,22]. Such reactions often start with low reaction rate. Fig. 4 shows three calculated isothermal and three calculated non-isothermal measurements in example 2 of Table 1. The initial phase of the reaction (30–45 s) cannot be measured precisely, as the steady state conditions are disturbed on introduction of the sample. However, the calculated initial rate at 30 °C is so slow that using a DSC the measured, distorted signal can be reliably corrected [11,20]. On the other hand the time (>6 h) taken to complete the reaction requires a device with very good long-term stability. Whereas the reaction at 70 °C is already so fast that a considerable part of this reaction occurs within the first 45 s, then each attempt to correct the initial heat flow rate must fail. In other words, the experimentally accessible temperature window for absolutely reliable isothermal measurements is relatively narrow (about 30–40 K).

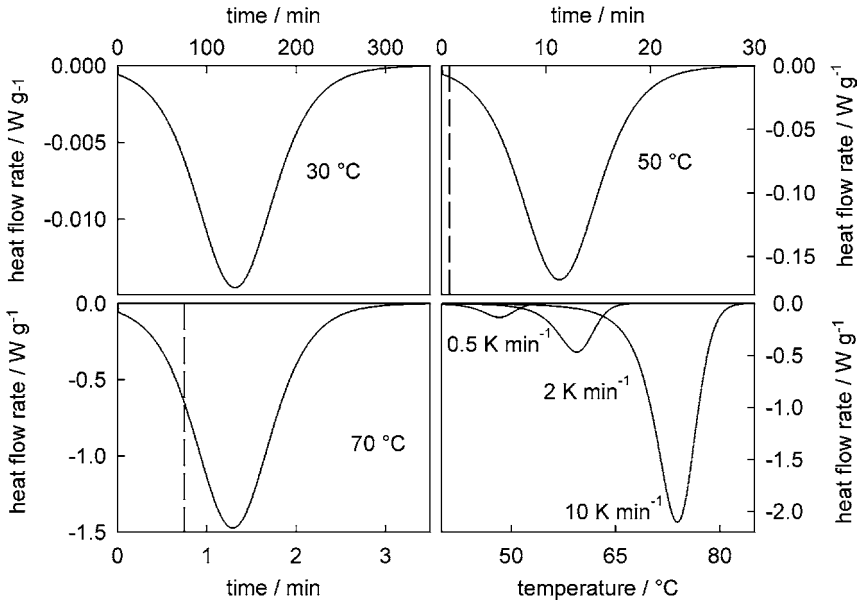

Fig. 4. Three calculated isothermal and three calculated non-isothermal (bottom right) curves of an autocatalytical second-order reaction (compare Table 1). Trustworthy experimental heat flow rates using isothermal conditions are only obtained for times longer than 0.75 min (the dashed line in the figures for 50 and 70 °C isotherms).

The situation becomes dramatic if an elementary step with an *n*th-order reaction ($n > 1$) dominates. This is shown in Fig. 5 for second-order kinetics (example 1 in Table 1). It is no longer possible to find a temperature range in which error-free measurements can be made: at temperatures higher than 25 °C the heat flow rate is strongly disturbed and falsified at the beginning; at temperatures lower than 25 °C, the end of the reaction cannot be detected because signal and noise will have the same magnitude. Again, non-isothermal runs are clearly favorable.

3.3. Comparison with already published cases

Two examples are to be discussed, the experimental details are described in our previous papers [21,23].

The first example is dimerisation of pure cyclopentadiene above room temperature [23]. This Diels–Alder reaction is autocatalysed and reaches a temperature-dependent equilibrium [23,24]. The most probable reaction mechanism is:

$$2\mathrm{CPD} \xrightarrow{k_1} \mathrm{DCPD} \qquad (2)$$

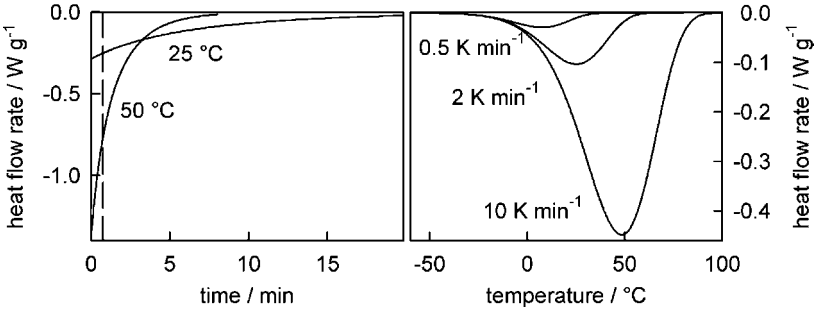

Fig. 5. Calculated isothermal and non-isothermal scans of a second-order reaction (compare Table 1and Fig. 4). Conclusion, the usable temperature range for isothermal measurements is extremely restricted in the case of (rate-determining) nth-order reactions ($n \neq 1$).

$$\mathrm{DCPD} \xrightarrow{k_2} 2\mathrm{CPD} \quad (3)$$

$$2\mathrm{CPD} + 1\mathrm{DCPD} \xrightarrow{k_3} 2\mathrm{DCPD} \quad (4)$$

where CPD is the monomer and DCPD is the dimer. In the past, we have evaluated the DSC measurements for this system using the program "NETZSCH Thermokinetics". This program allows the formal-kinetic description of a reaction, i.e. formal reaction steps instead of real elementary reactions. In a previous version of this program used in [23], autocatalytical reactions could only be described if two preconditions were assumed: a) the activation energy of the autocatalysed reaction was the same as that of the non-catalysed parallel reaction; b) only the pre-exponentials were different. The differential equation to be solved was then:

$$-\frac{\mathrm{d}c_{\mathrm{CPD}}}{\mathrm{d}t} = A_1 \exp\left(\frac{-E_{\mathrm{A1}}}{RT}\right) c_{\mathrm{CPD}}^2 (1 + K_{\mathrm{cat}} c_{\mathrm{DCPD}}) - A_3 \exp\left(\frac{-E_{\mathrm{A3}}}{RT}\right) c_{\mathrm{DCPD}} \quad (5)$$

The new program "Component kinetics" allows correct and unrestricted processing of the system of differential equations for the above mechanism. Fig. 6 shows the comparison between measured and calculated curves (for the sake of clarity, only one curve for each heating rate). Of course, the fit is not better than when using the formal-kinetic program [23], but the somewhat arbitrarily defined parameter "K_{cat}" in Eq. (5) is no longer needed and the kinetic parameters can be interpreted as usual. In addition, the new program allows the volume contraction during the reaction ($\varrho_{\mathrm{CPD}} = 0.7970\ \mathrm{g\ cm^{-3}}$, $\varrho_{\mathrm{DCPD}} = 0.9770\ \mathrm{g\ cm^{-3}}$) to be considered. Table 3 summarises the results of both types of kinetic evaluation. Due to the larger number of curves which can be treated in the new program (16 instead of 8), all measurements (one data set for the MDSC 2920 and two data sets for the DSC 2C) were loaded and evaluated simultaneously.

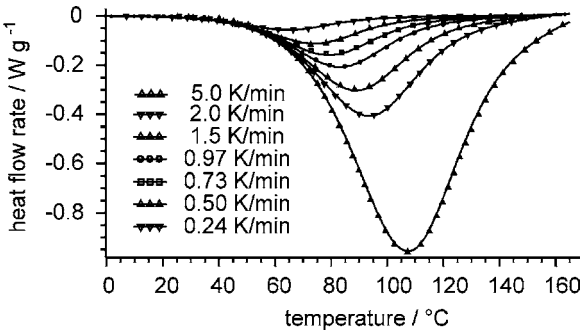

Fig. 6. Comparison between measured (symbols) and calculated (solid lines) curves for the CPD dimerisation.

The final example is very instructive. In an earlier paper [21], we reported results for the polyaddition reaction of bisphenol-A-diglycidyl ether (DGEBA) with the disecondary diamine *N*,*N*′-dibenzyl-4,4′-diaminodiphenymethane (DBMDA). At that time we could not analyse isothermal and non-isothermal scans simultaneously, assuming a certain reaction mechanism. The evaluation using the non-linear regression was restricted to isothermal scans for a number of stoichiometric and non-stoichiometric mixtures. The

Table 3
Comparison of the results of the kinetic analyses for the CPD-dimerisation according to Eqs. (2)–(4), using both formal-kinetic [23] and real kinetic evaluation. Compared with the earlier published standard deviations [23], all values were multiplied with the Durbin-Watson factor to yield a more realistic impression (see Appendix A in [11])

	Formal-kinetic evaluation, "NETZSCH Thermokinetics"			Real kinetic evaluation "component kinetics"
Parameter	Data set, MDSC 2920	Data set 1, DSC 2C	Data set 2, DSC 2C	All data sets
$\log A_1$ ($\mathrm{s^{-1}\,l\,mol^{-1}}$)	5.973 ± 0.40	5.942 ± 0.18	5.966 ± 0.30	5.74 ± 0.15
E_{A1} ($\mathrm{kJ\ mol^{-1}}$)	69.17 ± 2.5	69.01 ± 1.2	69.15 ± 1.50	69.43 ± 1.00
$\log (K_{\mathrm{cat}}/\mathrm{l\ mol^{-1}})$	0.022 ± 0.015	0.028 ± 0.01	0.029 ± 0.01	–
$\log A_2$ ($\mathrm{s^{-1}\,l\,mol^{-1}}$)	–	–	–	5.50 ± 0.30
E_{A2} ($\mathrm{kJ\ mol^{-1}}$)	–	–	–	73.79 ± 2.40
$\log A_3$ ($\mathrm{s^{-1}}$)	12.66 ± 1.6	13.21 ± 0.5	13.23 ± 0.8	13.04 ± 0.25
E_{A3} ($\mathrm{kJ\ mol^{-1}}$)	142.1 ± 12.2	142.0 ± 5.5	142.3 ± 7.6	142.0 ± 2.2
Correlation coefficient	0.9998	0.9997	0.9997	0.9997

most probable reaction model is to a large extent in accordance with the original suggestion of Smith [2]:

$$E + OH \overset{k_1}{\rightleftarrows} EOH \quad (6)$$

$$A + OH \overset{k_2}{\rightleftarrows} AOH \quad (7)$$

$$E + A \overset{k_1}{\rightarrow} AP + OH \quad (8)$$

$$EOH + A \overset{k_2}{\rightarrow} AP + 2OH \quad (9)$$

$$EOH + AOH \overset{k_3}{\rightarrow} AP + 3OH \quad (10)$$

where A is the amine, E the epoxide, OH the acid hydroxyls, AP the polyaddition product and AOH, EOH are hydrogen-bonded complexes.

Of course, the OH's of Eq. (8)–(10) are inseparable parts of the addition-polymer, but the kinetic evaluation is easier, if they are used as separate species. Assuming a fixed equilibrium constant for the forming of the $E \cdots OH$ complexes ($0.7\ l\ mol^{-1}$), as in other comparable systems [22,25], $K_{A\cdots OH} = 0.205\ l\ mol^{-1}$ was found. The three rate constants were determined for each temperature in the restricted temperature range between 400 and 460 K. Other possible reaction models clearly supplied worse fits. In particular, it was necessary to consider the last reaction step (Eq. (10)) as suggested first by Mijovic [26]. Nevertheless, the kinetic parameters obtained for the non-perfect measurements are only local solutions for the temperatures having been used. That means, the activation parameters using the Arrhenius equation are not necessarily the best values, particularly due to the extreme correlation between log A and E_A (kinetic compensation effect). In other words, the best local solution for the above isothermal measurement at a single temperature, containing individual and different errors, always yields a somewhat better fit than that of the global solution (multiple temperatures or multiple heating rates). As a rule, this is mostly only recognisable on the basis of the correlation coefficient (least squares) and not usually by visual comparison between experiment and fit.

Using the new evaluation program and the same mechanism, we have simultaneously re-evaluated the isothermal (400, 430 and 460 K) and the non-isothermal (0.8, 2 and $5\ K\ min^{-1}$) measurements of the system DGEBA/DBMDA. The activation parameters for the global solution obtained are compared with the old values in Table 4. The reason for the distinct variations between the kinetic parameters for one and the same reaction is the compensation effect, as already discussed. As shown in Fig. 7, the new activation parameters are also consistent with the conversion-dependent E_A-values, resulting from the model-free evaluation of all isothermal and non-isothermal measurements (circles). If only the isothermal measurements are taken into account (triangles), then the dependence of E_A corresponds better with the old values.

Table 4
System DGEBA/DBMDA; kinetic parameters according to the reactions (6)–(10), K_1 = constant = $0.7\ l\ mol^{-1}$, K_2 = constant = $0.205\ l\ mol^{-1}$. Old: activation parameters from the evaluation of the isothermal scans at 400, 430 and 460 K. New: activation parameters from the simultaneous evaluation of both isothermal (400, 430 and 460 K) and non-isothermal scans (0.8, 2.0 and $10.0\ K\ min^{-1}$)

Parameter	Old	New
$\log A_3$ ($s^{-1}\ l\ mol^{-1}$)	4.54 ± 0.50	5.03 ± 0.33
E_{A3} ($kJ\ mol^{-1}$)	71.9 ± 5.1	76.2 ± 2.8
$\log A_4$ ($s^{-1}\ l\ mol^{-1}$)	3.88 ± 0.52	3.21 ± 0.25
E_{A4} ($kJ\ mol^{-1}$)	57.8 ± 4.8	52.3 ± 2.1
$\log A_5$ ($s^{-1}\ l\ mol^{-1}$)	3.00 ± 0.66	4.07 ± 0.37
E_{A5} ($kJ\ mol^{-1}$)	45.5 ± 5.9	54.6 ± 3.2
Correlation coefficient	0.9978	0.9990
Weighted least squares	0.3767	0.1903

The new program also allows the output of the concentrations of all components for any reaction conditions. This is shown in Fig. 8 for the last system. For the sake of clarity, only the concentrations of the

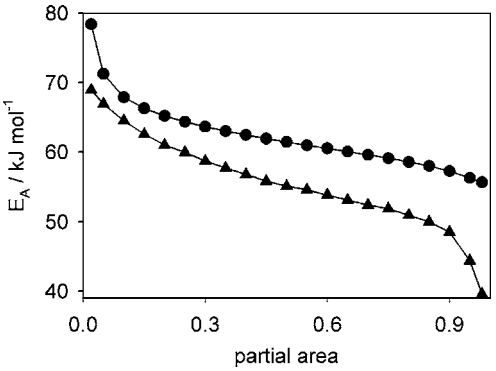

Fig. 7. System DGEBA/DMBA, model-free estimation of the activation energy. Circles: isothermal and non-isothermal measurements, Triangles: only isothermal runs.

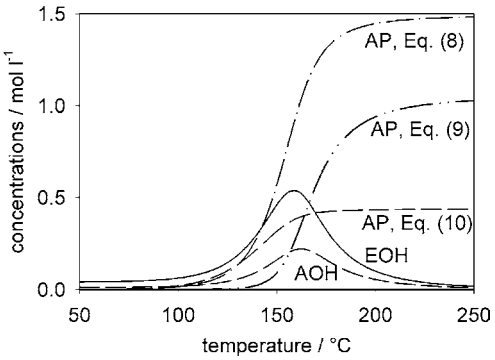

Fig. 8. System DGEBA/DBMDA, heating rate : 0.8 K min^{-1}, concentration profiles of the EOH- and AOH-complexes and of the addition polymer AP produced according to the three possible routes (according to Eqs. (8–10)), initial concentrations: $c_E = c_A = 2.98$ mol l^{-1}, $c_{OH} = 0.075$ mol l^{-1}.

OH-complexes and those of the reaction products produced during the three different reaction steps (Eqs. (8)–(10)) are shown. Mijovic's arguments [26] that the route according to Eq. (10) is only active above a critical concentration of the hydroxyl groups must now be modified. It does not reach a distinct significance until sufficient hydroxyl groups are formed (hence, AOH and EOH complexes). Nevertheless, a kinetic model must consider this new route during the entire reaction.

4. Conclusions

The new program removes one of the main disadvantages of previous evaluation programs: the restriction to systems with a fixed stoichiometric composition. The simultaneous evaluation of DSC curves, belonging to systems with different initial compositions, is extremely important for two reasons. Firstly, variable compositions of technical formulations, including possible solvent contents, are more the rule than the exception. Secondly, searching for or verifying the most probable reaction mechanism ideally requires the screening of the complete global reaction field. The evaluation of multiple heating scans should be a matter of course [13,15]. For the same reason it is necessary to use different initial concentrations in order to investigate more complex reaction mechanisms.

It was shown that the program operates correctly for all possible combinations of elementary reactions and equilibrium steps in homogeneous kinetics when using error-free, calculated DSC curves. Without exception, the global minimum is found after very few iterations. The kinetic parameters and reaction heats exactly reproduce the theoretical values, presupposing that the correct model is used.

Two typical sources of error in DSC experiments have very different consequences for the correctness of the model parameters determined. Noisy curves produce negligible errors. On the other hand, undetected jumps, uncorrected base line curvatures and non-linear shifts between starting and end point of the measurements are very critical. In the extreme case, it is then impossible to find the significantly best and chemically reasonable model, or an erroneous sequence of steps is interpreted as being the true mechanism. This risk can only be diminished by using repeated scans, obtained under apparently identical measuring conditions. Further, base line constructions or better independent base line measurements must be carried out with the greatest possible care.

When planning measurements for a kinetic evaluation, the selection of the proper window in the global temperature-time-concentration space is extremely important. Therefore, temperature-programmed experiments should be carried out using very different heating rates. At least three (better 5) measurements should be made in the range between 0.5 and 10 K min^{-1}. This requirement should cause no practical problems. Using the correct kinetic model, the kinetic parameters obtained should then also adequately describe isothermal scans. This can be regarded as a test procedure concerning the correctness of the model. But the best way is always to include some isothermal experiments into the kinetic evaluation. Using only isothermal measurements cannot be recommended. Apart from a few reactions with very simple mechanisms, the experimentally accessible reaction window is much too small for reliable calculations.

Numerous advantages of the new program are discussed above. For example, unrestricted validity of the results for any initial compositions including different amounts of catalysts, solvents and non-reactive fillers, inclusion of equilibrium reactions, considerations of volume changes during the reaction. But one disadvantage should not be concealed. It is much

more time consuming when compared to a formal-kinetic evaluation. This concerns both the measurements (sometimes including additional and necessary information from other analytical techniques) and the non-linear regression itself. The user has to estimate the cost-benefit ratio. If the aim is not to find the ''true'' mechanism but only to find a model which describes the behavior of a just investigated reaction mixture as well as possible, then a formal-kinetic evaluation is easier and much faster. The fit to the experimental curves is usually just as good. On the other hand, more complicated tasks are naturally more time-consuming, but this is not typical for the program presented here.

References

[1] S. Sourour, M.R. Kamal, Thermochim. Acta 14 (1976) 41.
[2] I.T. Smith, Polymer 2 (1961) 95.
[3] M.E. Ryan, A. Dutta, Polymer 20 (1979) 203.
[4] T.S. Chung, J. Appl. Polym. Sci. 29 (1984) 4403.
[5] M.R. Keenan, J. Appl. Polym. Sci. 33 (1987) 1725.
[6] H. Friedman, J. Polym. Sci. Part C 6 (1965) 183.
[7] T. Ozawa, Bull. Chem. Soc. Jpn. 38 (1966) 1881.
[8] J.H. Flynn, L.A. Wall, Polym. Lett. 4 (1966) 232.
[9] S. Vyazovkin, Int. J. Chem. Kinet. 28 (1996) 95.
[10] J. Opfermann, F. Giblin, J. Mayer, E. Kaisersberger, American Laboratory February 1995, p. 1.
[11] H.J. Flammersheim, Thermochim. Acta 361 (2000) 21.
[12] H.J. Flammersheim, J. Opfermann, Macromol. Mater. Eng. 286 (2001) 143.
[13] B. Roduit, Thermochim. Acta 355 (2000) 171.
[14] J. Opfermann, J. Therm. Anal. Cal. 60 (2000) 641.
[15] A.K. Burnham, Thermochim. Acta 355 (2000) 165.
[16] G. Engeln-Müllges, F. Reuter, Numerik-Algorithmen, VDI Verlag GmbH, Düsseldorf, 1996.
[17] P.D.M. Benoit, R.G. Ferillo, A.H. Ganzow, Anal. Chim. Acza 124 (1985) 869.
[18] S. Vyazovkin, Thermochim. Acta 355 (2000) 155.
[19] M. Reading, A. Luget, R. Wilson, Thermochim. Acta 238 (1994) 295.
[20] G. Höhne, W. Hemminger, H. J. Flammersheim, Differential Scanning Calorimetry, Springer, Berlin, 1996, pp. 143–146.
[21] J. Klee, R.E. Grützner, H.H. Hörhold, H.J. Flammersheim, Macromol. Chem. Phys. 199 (1998) 153.
[22] H.J. Flammersheim, Thermochim. Acta 310 (1998) 153.
[23] H.J. Flammersheim, J. Opfermann, Thermochim. Acta 337 (1999) 149.
[24] A.G. Turnbull, H.S. Hull, Aust. J. Chem. 21 (1968) 1789.
[25] B.A. Rozenberg, Adv. Polym. Sci. 75 (1986) 113.
[26] J. Mijovic, A. Fishbain, J. Wijaya, Macromolecules 25 (1992) 979.